NEUROSCIENCE

10.1126/sciadv.1501733

Bidirectional radial Ca^{2+} activity regulates neurogenesis and migration during early cortical column formation

Brian G. Rash,[1] James B. Ackman,[1,2] Pasko Rakic[1,3]*

Cortical columns are basic cellular and functional units of the cerebral cortex that are malformed in many brain disorders, but how they initially develop is not well understood. Using an optogenetic sensor in the mouse embryonic forebrain, we demonstrate that Ca^{2+} fluxes propagate bidirectionally within the elongated fibers of radial glial cells (RGCs), providing a novel communication mechanism linking the proliferative and postmitotic zones before the onset of synaptogenesis. Our results indicate that Ca^{2+} activity along RGC fibers provides feedback information along the radial migratory pathway, influencing neurogenesis and migration during early column development. Furthermore, we find that this columnar Ca^{2+} propagation is induced by Notch and fibroblast growth factor activities classically implicated in cortical expansion and patterning. Thus, cortical morphogens and growth factors may influence cortical column assembly in part by regulating long-distance Ca^{2+} communication along the radial axis of cortical development.

INTRODUCTION

The cerebral cortex is an array of interacting, cytoarchitecturally diverse radial columns (*1*). The instructions that build these columns during embryonic development are rooted in the proliferative zones and then translated into columnar pattern via precise radial migration, establishing order and exquisite connectivity between participating neurons (*2*–*8*). Although the concept that radial migration leads neurons from their place of origin to proper columnar, laminar, and areal locations in the developing cortex is over four decades old (*2*, *8*), little is known about the communication mechanisms coordinating neuronal migration within developing cortical columns before the establishment of synapses. In particular, the source of radial information along the migratory pathway of excitatory neurons remains unknown.

Positional information in the tangential dimension can take the form of protein gradients (morphogens) and may also use cell-cell adhesion molecules, or it may be encoded by patterns of neural activity. For example, the pattern of functional areas in the mature cortex is set up by the area protomap, which is governed by diffusible morphogens such as fibroblast growth factors (FGFs) (*2*, *9*, *10*). Subsequently, patterns of spiking cortical activity originating from peripheral sensory organs play a key role in synaptic development of sensory cortical maps (*11*, *12*).

A key step in the radial development of the cortex is the exit of newborn neurons from the proliferative ventricular zone (VZ), which begins with apical end-foot retraction and the initiation of radial neuronal migration (*13*, *14*). Consequently, migrating neurons become isolated from factors present in the stem cell niche and become exposed to other signals, although they have not yet formed synaptic connections. Thus, one may hypothesize the existence of nonsynaptic communication in the radial dimension, which may (i) be used by migrating neurons to establish proper laminar order, (ii) provide a feedback mechanism between the proliferative and postmitotic zones, influencing proliferation and neurogenesis, and (iii) be regulated by morphogens and growth factors during development. One possible conduit for radial communication is the elongated fiber of radial glial cells (RGCs), but no mechanism for information transfer influencing column formation has been described. Here, we found that patterned Ca^{2+} activity can fill this role.

[1]Department of Neuroscience, Yale University, New Haven, CT 06520, USA. [2]Department of Molecular, Cell, and Developmental Biology, University of California, Santa Cruz, Santa Cruz, CA 95064, USA. [3]Kavli Institute for Neuroscience, Yale University, New Haven, CT 06520, USA.
*Corresponding author. E-mail: pasko.rakic@yale.edu

RESULTS

Radial calcium activity in developing cortical columns

Calcium flux directly regulates key cellular behaviors, including proliferation, interkinetic nuclear migration, and neurite extension in many model systems, including the developing cerebral cortex, and also regulates the expression of certain Ca^{2+}-responsive genes (*15*–*19*); for review, see the study by Webb and Miller (*20*) and by Berridge (*21*). Specific frequencies of Ca^{2+} transients induce cellular events that mediate specific aspects of these processes (*22*). Moreover, specific cellular compartments generate unique Ca^{2+} transient activities that, for example, regulate the rate of growth cone extension in developing *Xenopus* spinal axons (*23*).

Calcium transient activity is exhibited by early neural progenitor cells and is thought to regulate proliferation (*17*–*19*), but its role in cortical column development has not been investigated. RGCs are morphologically very specialized, and we hypothesized that their elongated fibers, extending to the apical and pial surfaces, are likely to require soma-independent regulation of local Ca^{2+} flux, similar to axons and dendrites (*24*–*27*). The analysis of Ca^{2+} activity in fine cellular structures such as thin RGC fibers requires a cell type–specific, high-resolution method other than the traditional, nonspecific, bath-applied Ca^{2+} dyes used in cortical slice cultures. Here, we labeled RGCs with an optogenetic sensor—GCaMP5G (*28*)—using in utero electroporation (IUE) between E10.5 and E14.5 and recorded the Ca^{2+} dynamics of RGC fibers via confocal and two-photon videomicroscopy,

using ex vivo and slice preparations. Only RGCs are labeled by IUE (*29*), and we limited survival time to 16 to 18 hours to minimize differentiation, ensuring that, essentially, all labeled cells are RGCs. This permits specific labeling and clear identification of RGC fibers, as well as high sensitivity detection of their Ca^{2+} transient activity.

Cortical neurogenesis begins around E11.0 in the mouse, but newborn neurons are not organized into columns until later in development when RGC fibers act as migration guides (*4*). At E15.5, when the RGC scaffold is fully developed, we found that the elongated fibers of RGCs showed prominent Ca^{2+} transients traveling long distances in developing cortical columns (Fig. 1, A to C, E, G, and I, and video S1). Calcium transients were abundant in both RGC cell bodies and fibers throughout the period of cortical neurogenesis, between E11.0 and E18.5. Radial fiber Ca^{2+} transients were often single events, but some exhibited rapid bursting behavior (Fig. 1, F, H, and J, and video S2), demonstrating that RGC fibers can modulate the frequency of propagative information like cell somata in other contexts (*30*).

Many of these Ca^{2+} transients occurred independent of cell body activity and were either propagative (>10-μm fiber segments active) or nonpropagative. Nonpropagative Ca^{2+} transients (NPCTs) were generally displayed by small puncta along the length of the RGC fiber, which usually correspond with varicosities or lamellate expansions (Fig. 1 and video S2). Propagative Ca^{2+} transients (PCTs) originated from any point along RGC fibers, including apical and basal end feet, and were often bidirectional, proceeding anterogradely and retrogradely from the point of origin with an average velocity of 10.6 ± 1.4 μm/s (n = 13). Some PCTs were unidirectional. The mean propagated distance for PCTs was 59.8 ± 4.1 μm (n = 56 events from three embryos), but some PCTs were observed to span the distance from the ventricular surface to the MZ (Fig. 1C and video S1). The majority of RGC fiber Ca^{2+} transients were propagative (88.62 ± 3.18% PCTs versus 11.38 ± 3.18% NPCTs, $P < 0.0001$, n = 295 events from three embryos). Propagative RGC fiber transients initiated in the intermediate zone (IZ), cortical plate (CP), or MZ were categorized as 18.7% anterograde, 37.4% retrograde, and 44.0% bidirectional. A majority of total Ca^{2+} transients in the IZ, CP, or MZ (83.8%) were either retrograde, bidirectional, or nonpropagative and were therefore considered to be initiated independent of the RGC soma. Ca^{2+} transients originated in the cell body and propagated long distances anterogradely through both apical and basal fibers, with some reaching the pial surface (fig. S1 and videos S3 and S4). Other transients originated in the RGC fiber and propagated retrogradely to activate the RGC cell body (video S5). Pial end feet displayed the highest level of Ca^{2+} activity within basal RGC fibers and were capable of initiating retrograde PCTs (Fig. 2 and video S6), but apical end feet showed the highest frequency of Ca^{2+} transients within RGCs, and the VZ was the most active overall zone in the cortical wall (n = 1497 Ca^{2+} events from N = 4 E15.5 slices; fig. S2). Unexpectedly, we also detected

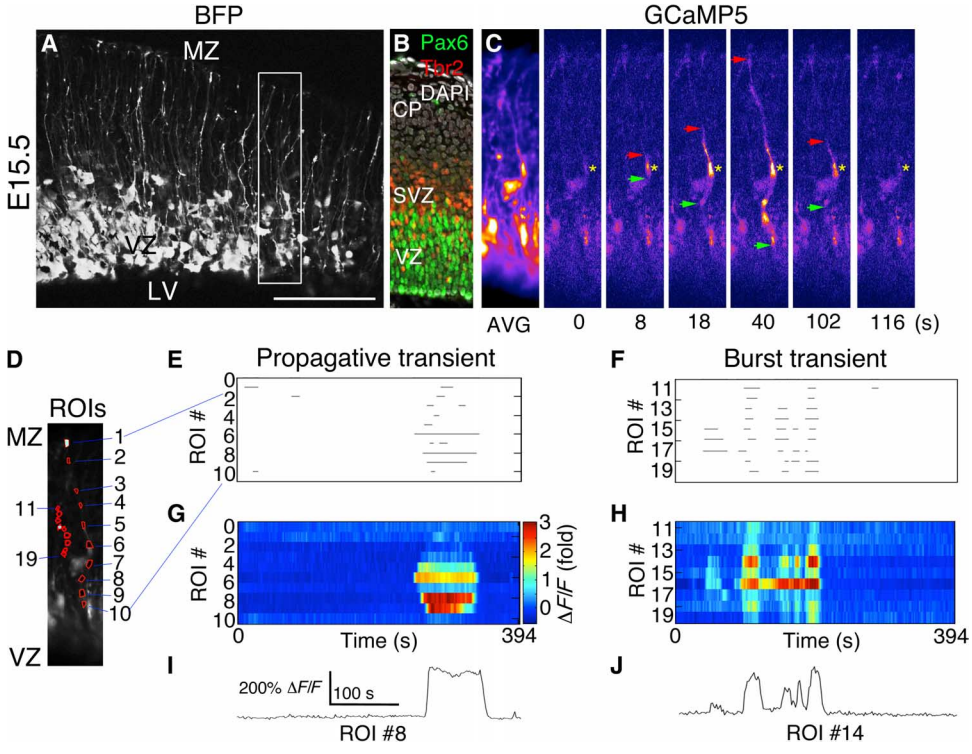

Fig. 1. PCTs in RGC fibers during neurogenesis. (**A**) Blue fluorescent protein (BFP) *Z*-stack of a live E15.5 mouse cortical slice from an embryo coelectroporated with pCAG-BFP and pCAG-GCaMP5G at E14.5. (**B**) Immunohistochemistry to visualize VZ and SVZ (subventricular zone) at the time of electroporation. DAPI, 4′,6-diamidino-2-phenylindole. (**C**) Time-lapse images corresponding to the boxed region in (A) showing a Ca^{2+} transient originating in an RGC fiber segment (yellow asterisk) and propagating bidirectionally (red and green arrows). AVG, average. (**D**) Regions of interest (ROIs) corresponding to two separate Ca^{2+} events in the same movie, drawn in MATLAB. (**E** to **H**) Ca^{2+} event properties were extracted from Ca^{2+} movies and rendered as rasterplots or heat map intensity plots. (**I** and **J**) Ca^{2+} activity traces for individual ROIs showing single or burst Ca^{2+} transients in RGC fibers. LV, lateral ventricle; MZ, marginal zone. Scale bars, 125 μm (A) and 100 μm (B and C).

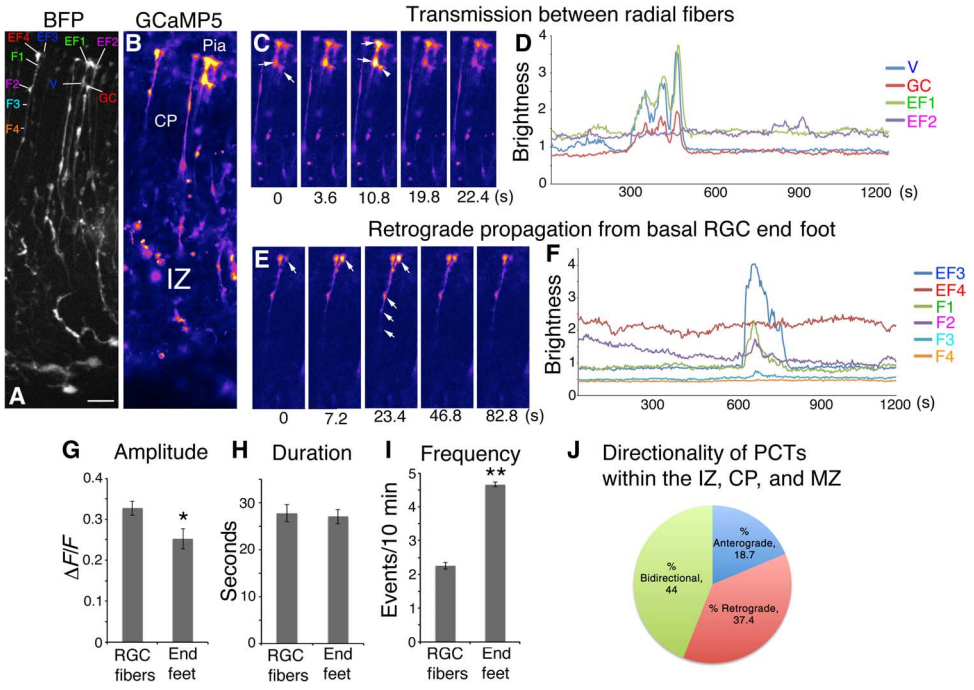

Fig. 2. Calcium transient activity and directionality in RGC fibers and pial end feet. (**A**) BFP *Z*-stack of RGC fibers. (**B**) Corresponding image of GCaMP5 fluorescence. (**C**) Time-lapse images of coherent activity in two RGC end feet. (**D**) Calcium activity traces of the series in (C); note that the multiple fluorescence events of a growth cone (GC) of an adjacent RGC fiber accurately mirror activity of the adjacent end foot. (**E**) Time-lapse series of pial end foot initiating a Ca^{2+} transient, which propagates retrogradely through the CP. (**F**) Calcium activity traces for the series in (E) showing temporal progression of the Ca^{2+} wavefront in the RGC fiber. (**G** to **I**) Population comparison of Ca^{2+} event properties within RGC fibers and pial end feet showing respective amplitude, duration, and frequency. (**J**) PCTs originating in the IZ, CP, and MZ categorized by directionality. Note that MZ transients may be nonpropagative or retrograde only. EF1 to EF4, end foot 1 to end foot 4; V, varicosity; F1 to F4, fiber point 1 to fiber point 4. *$P < 0.05$; **$P < 0.001$. Error bars, mean ± SEM. Scale bar, 20 μm.

an inverse relationship between Ca^{2+} event frequency and amplitude along radial fibers; amplitude increases toward the pial surface, whereas frequency decreases (fig. S2).

Although only a small fraction of RGCs were labeled by GCaMP5 electroporation, we found coherent activity in localized clusters of up to seven RGC fibers, spanning cortical regions up to approximately 50 to 100 μm wide (Fig. 3, A to H, and video S7). The clusters of RGC fibers showed significant correlation in their activity patterns ($P < 0.01$) (Fig. 3C). This could represent shared Ca^{2+} activation mechanisms within a single cortical column or multiple columns firing in synchrony. Plotting orientation direction lines from correlated ROI pairs on polar coordinates confirmed that correlations were predominantly radial, reflecting radial propagation of Ca^{2+} transients along radial fibers (Fig. 3E). We also observed correlated Ca^{2+} activity among adjacent RGC pial end feet (Fig. 2 and video S8). Repeated RGC fiber-fiber correlated events were observed throughout the thickness of the cortical wall, including the CP and IZ (video S9). Adjacent cells, such as postmitotic neurons and other RGC fibers (not visible), do not contain GCaMP5 but are expected to participate in such events and may trigger the visible coherent activity in GCaMP5-labeled RGC fiber clusters. Together, these data strongly suggest shared activational mechanisms involving diffusible ligand-receptor systems or direct RGC fiber-fiber communication, possibly by gap junctions (*15*, *31*, *32*).

To investigate the origin of Ca^{2+} ions during propagative transients in RGC fibers, we exposed slices to Ca^{2+}-free artificial cerebrospinal fluid (ACSF) alone or in combination with 2-aminoethoxydiphenyl borate (2-APB), which inhibits inositol 1,4,5-trisphosphate (IP_3) receptor (IP_3R)–mediated Ca^{2+} release from endoplasmic reticulum. RGC fibers exhibited a similar response to RGC cell bodies, including a marked reduction of Ca^{2+} transient amplitude and frequency due to 100 μM 2-APB ($n = 1588$ events from $N = 4$ control slices; $n = 3170$ events from $N = 4$ Ca^{2+}-free slices; $n = 786$ events from $N = 2$ Ca^{2+}-free + 2-APB slices) (Fig. 3, I to K). The duration of events was not significantly altered in either case. Both RGC cell bodies and fibers showed increased event amplitude and frequency during exposure to Ca^{2+}-free ACSF, indicating a partial dependence on extracellular Ca^{2+} concentration.

Ca^{2+} activity bursts during differentiation and radial neuronal migration

During the earliest stages of neurogenesis, RGCs may first undergo mitosis at the ventricular surface, or they may retract their apical process and then differentiate directly (*4*, *33*). The newly differentiating cell exits the VZ and may proceed directly to the CP as a newborn neuron, or it may enter a multipolar stage of further cell division in the SVZ (*3*, *34*). Previous studies demonstrated that early migrating granule neurons in the cerebellum depend on Ca^{2+} activity to regulate their migratory speed (*35*). To determine whether Ca^{2+} activity plays a role in specific events during neurogenesis and neuronal migration in the developing cortex, we examined long (1 to 3 hours) Ca^{2+} movies for neuroblasts exiting the VZ. We found that newly differentiating neuroblasts enter a phase of high-frequency Ca^{2+} activity immediately upon RGC end-foot retraction, as they begin to exit the VZ (Fig. 4, A

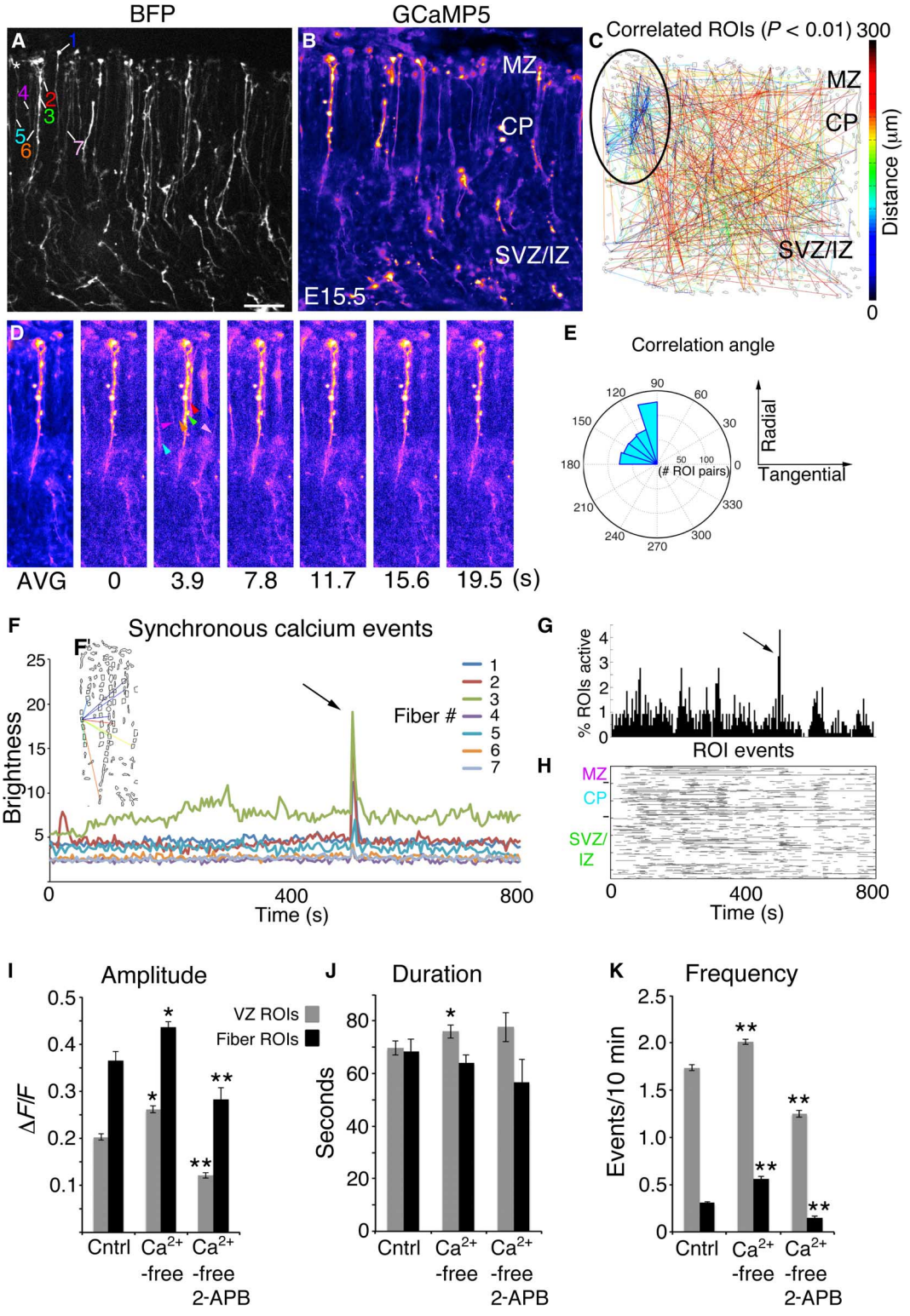

Fig. 3. Radial glial fibers form synchronous activation groups. (**A**) BFP Z-stack of an E15.5 cortical slice. (**B**) Averaged GCaMP5 movie. (**C**) Correlation map; clustered correlations indicated by black oval. (**D**) Time-lapse series; coherently active RGC fibers are indicated by colored arrowheads. (**E**) Correlation angles from correlated pairs in (C) binned and plotted on polar coordinates. (**F**) Absolute brightness traces from ROIs of coherently active RGC fibers. (**F′**) Correlated pairs within the synchronous cluster. (**G** and **H**) Extraction of Ca^{2+} event properties in MATLAB revealed the synchronous firing event in percent active and rasterplot form. (**I** to **K**) RGC cell body (gray bars) and fiber (black bars) activity in control (Cntrl) ACSF, Ca^{2+}-free ACSF, and Ca^{2+}-free ACSF plus 100 μM 2-APB. *$P < 0.05$; **$P < 0.001$, *t* test. Error bars, mean ± SEM. Scale bar, 40 μm.

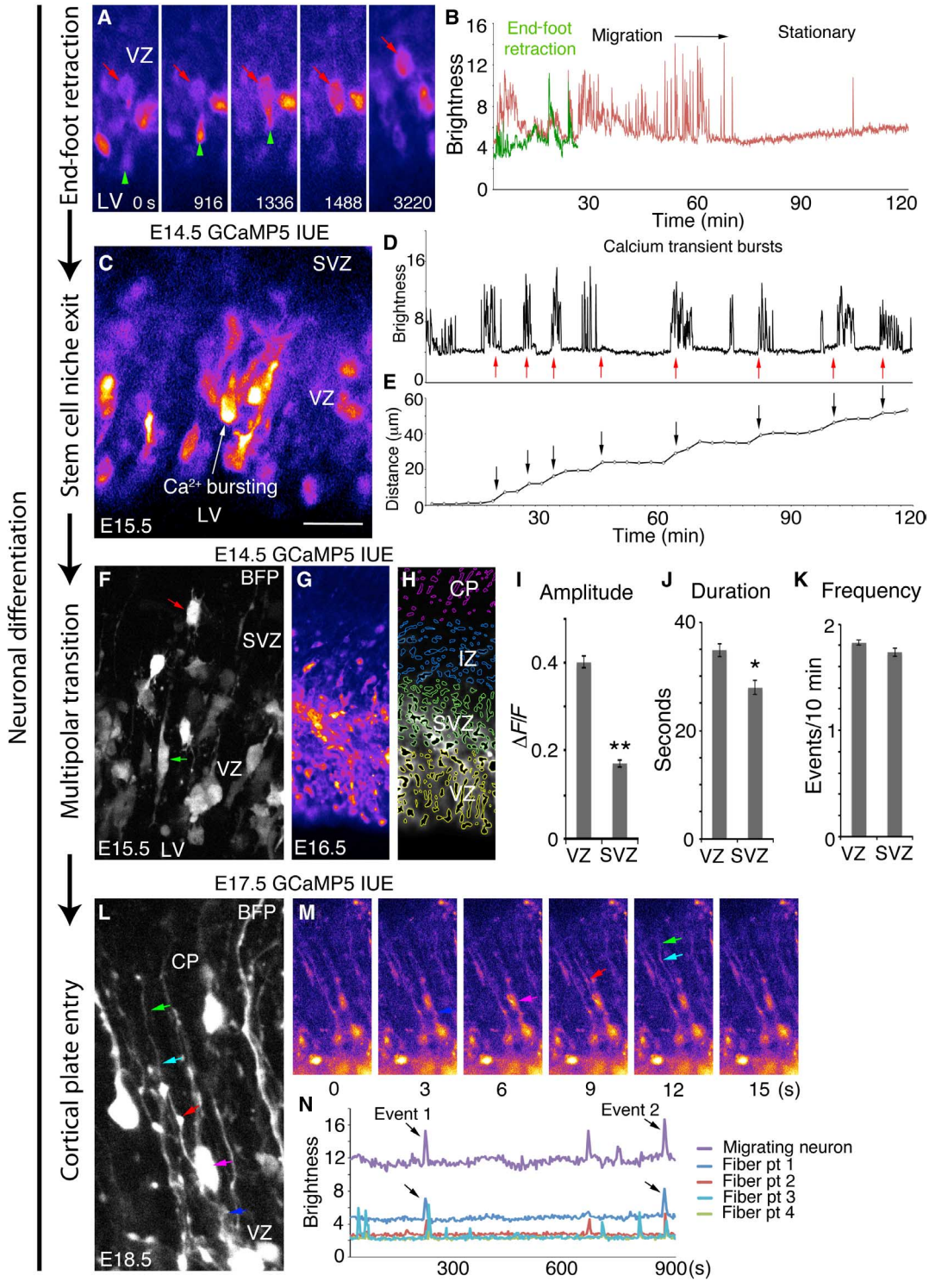

Fig. 4. Bursting calcium activity in newborn migrating neurons and communication with RGC fibers. (**A**) Retracting apical end foot (green arrowhead) and its cell body (red arrow). (**B**) Calcium activity traces of the cell in (A). (**C**) Putative migrating neuron exiting the VZ. (**D**) Calcium bursting activity (red arrows) of cell indicated in (C). (**E**) Distance traveled by cell in (C) (arrows) corresponding to Ca^{2+} bursts in (D). (**F**) BFP Z-stack showing electroporated RGCs (green arrow) and multipolar progenitors (red arrow). (**G**) GCaMP5G image of an E16.5 cortical slice after E14.5 electroporation. (**H**) MATLAB ROIs organized in embryonic zones corresponding to the image in (G). (**I** to **K**) Ca^{2+} activity properties of the VZ and SVZ. (**L**) BFP Z-stack of an RGC fiber (dark blue, red, light blue, and green arrows) and adjacent migrating neuron (magenta arrow) at E18.5. (**M**) Time-lapse GCaMP5 images of the cell in (L). (**N**) Correlated Ca^{2+} activity of the RGC fiber and neuron in (L) and (M). *$P < 0.05$; **$P < 0.001$, *t* test. Error bars, mean ± SEM. Scale bars, 25 μm (A, C, F, and L) and 80 μm (G and H).

to E, and video S10). Ca^{2+} activity was also exhibited by retracting apical end feet independent of RGC soma activity. Differentiating cells at this stage show the highest frequency of Ca^{2+} transients of any cell type in the developing cortex, taking on a classic migratory pear shape and rapidly exiting the VZ, sometimes in small localized groups, following their leading process radially toward the pial surface (Fig. 4C). To determine the role of IP_3R-dependent calcium activity on neuronal migration, we exposed slices to 2-APB and examined cell motile behaviors in relation to Ca^{2+} bursting. We observed 21 Ca^{2+} burst events from n = 1496 VZ ROIs in N = 12 control movies totaling 229 min and 0 Ca^{2+} burst events from 1022 VZ ROIs in N = 5 2-APB movies totaling 130 min. Most VZ ROIs corresponded to RGC cell bodies (88.64 ± 8.0%, n = 1469 ROIs from N = 12 slices), whereas the remainder corresponded to apical end feet or RGC fiber ROIs. Overall, there were 1.41 ± 0.174 Ca^{2+} burst events per RGC cell body per day in control movies versus 0 ± 0 during 2-APB exposure (P < 0.0001). In addition, we observed reduced RGC radial polarity and markedly decreased general motility and filopodial exploration during 2-APB exposure (video S11). Together, these data support the hypothesis that Ca^{2+} bursting may be needed for neuronal VZ exit/induction of radial migration.

We next found that bursts of Ca^{2+} transients accompanied and preceded nuclear translocation movements (Fig. 4, D and E, and video S12). As shown here, nondifferentiating RGCs exhibited both anterograde and retrograde nuclear translocation but no Ca^{2+} bursting. Upon exit from the VZ, many differentiating neuroblasts exhibited multipolar morphology in the SVZ; these cells showed reduced amplitude and duration of Ca^{2+} events, but SVZ and VZ event frequencies were similar (Fig. 4, F to K).

Unexpectedly, we observed repeated en passant transit of Ca^{2+} events in RGC fibers apparently inducing Ca^{2+} responses in adjacent migrating neurons (Fig. 4, L to N, and videos S13 and S14), indicating that RGC fibers can promote Ca^{2+} activity in differentiating neurons at a considerable distance from the RGC soma. At late stages of migration, Ca^{2+} transients in migrating neurons were generally less frequent and show lower amplitude (fig. S3). Together, these data indicate that Ca^{2+} activity may play specific regulatory or permissive roles in RGC fibers and migrating neurons during each stage of migration.

Whether Ca^{2+} transient activity occurs in the early cortical primordium of a live mouse embryo has not yet been established. Using IUE of plasmids encoding GCaMP5G and a membrane-targeted BFP at E10.25 followed by 14 hours of survival in utero, we labeled cortical progenitor cells and imaged their Ca^{2+} dynamics ex vivo at E11.0. We observed prominent Ca^{2+} dynamics in the cell bodies and early radial fibers of 405 neuroepithelial cells and early RGCs (fig. S4 and video S15). Although labeled cells were generally separated by several cell diameters, one adjacent pair of RGC precursors exhibited coactive patterns of Ca^{2+} transients. This is the first direct observation of Ca^{2+} transient activity in RGCs within live mouse embryos during cortical development and indicates that Ca^{2+} dynamics feature prominently even at the earliest stages of cortical neurogenesis.

Radial Ca^{2+} propagation induced by FGF and Notch

Embryonic signaling proteins such as FGFs and Notch are well known to control proliferation and differentiation of neural stem cells (*14*, *36*). FGF signaling, in particular, has been demonstrated to increase RGC proliferation and cause primary gyrification of the mouse cortex (*37*, *38*). However, Ca^{2+} activity has also previously been shown to increase proliferation rate (*17*, *19*). Therefore, we investigated whether Ca^{2+} dynamics might be directly regulated by these morphogenetic factors during cortical column formation.

We found that bath application of FGF2 protein (1 ng/μl) substantially increased the amplitude, duration, and frequency of Ca^{2+} events in RGC cell bodies within 30 s of exposure (n = 3584 total Ca^{2+} events from N = 4 slices; n = 2284 VZ Ca^{2+} events; Fig. 5, A to C, E to G, I to K, M, N, and P, and videos S16 and S17). Note that cortical gyrification was achieved in the mouse cortex with an FGF2 dosage 100-fold higher (*38*). The percentage of ROIs active in a 10-min recording increased from 28.6 ± 2.65% to 42.2 ± 4.08% (N = 4 slices, P < 0.05). Remarkably, the increased Ca^{2+} activity was first evident in RGC apical end feet positioned at the ventricular surface, and the activity progressed toward the pial surface through RGC fibers. RGC cell bodies showed peak Ca^{2+} activation within 5 min of FGF2 exposure. Between 16 and 26 min after FGF2 exposure, RGC cell bodies showed reduced duration and frequency consistent with a refractory period, whereas RGC fibers maintained a higher frequency of Ca^{2+} events (Fig. 5, D, H, I, L, O, and P). In summary, FGF2 increased the total number of events (Fig. 5, Q, S, and T) and Ca^{2+} propagation distance in RGC fibers from 59.8 ± 3.51 μm to 76.2 ± 3.31 μm (n = 56 control events, n = 113 FGF2 events from four slices, P < 0.05, Fig. 5R and videos S18 and S19).

Conversely, after 1 hour of exposure to PD173074, a relatively specific FGF receptor (FGFR) blocker (*39*), the amplitude of calcium signals was decreased in RGC cell bodies from 0.3155 ± 0.0112 $\Delta F/F$ to 0.2227 ± 0.00745 $\Delta F/F$ (P < 0.0001, n = 929 control events and n = 1033 PD173074 events, N = 3 slices, fig. S5). Amplitude was similarly decreased in RGC cell bodies, although the duration and frequency of Ca^{2+} events was only modestly affected, if at all, in RGC cell bodies and fibers. Together, these data indicate that FGFR activity partly regulates Ca^{2+} transient event properties in cortical slices isolated from their primary source of FGF ligands—the rostral telencephalic midline, which is a major source of FGFs including FGF8, FGF17, and FGF18 (*40*). Degradation of Ca^{2+} activity via PD173074 likely reflects either (i) reduction of intrinsic signaling activity of FGFRs in the absence of FGF ligand, (ii) reduction of FGFR activity due to endogenous FGF2 expression previously reported in the VZ (*41*), or both.

Notch activity is also a major determinant of proliferation and differentiation of stem cells in many model systems, including the developing cortex (*36*), and is activated in cortical RGCs by FGF signaling (*37*, *38*). Studies have indicated that extracellular Ca^{2+} influences the activation of the downstream Notch targets Hes1 and Hey1 (*42*). To test the hypothesis that Notch activity reduces the Ca^{2+} bursting activity in RGCs, leading to neurogenesis, we coelectroporated a plasmid encoding the active NICD along with BFP and GCaMP5G. The NICD plasmid activates downstream Notch targets including Hes1 in RGCs and promotes their proliferation (*37*). NICD electroporation effectively abolished Ca^{2+} bursting activity in the VZ (Fig. 5, U and V; n = 27 control burst migrations, all of which were pear-shaped putative newborn neurons, versus only a single instance observed with NICD electroporation). NICD electroporation increased the overall amplitude and frequency of VZ Ca^{2+} transients (n = 4837 Ca^{2+} events from four control slices; n = 6325 Ca^{2+} events from four NICD slices; Fig. 5, W to Y, and video S20). This indicates that regulation of Ca^{2+} activity is an integral component of Notch function in regulating initial stages of cortical neurogenesis and migration.

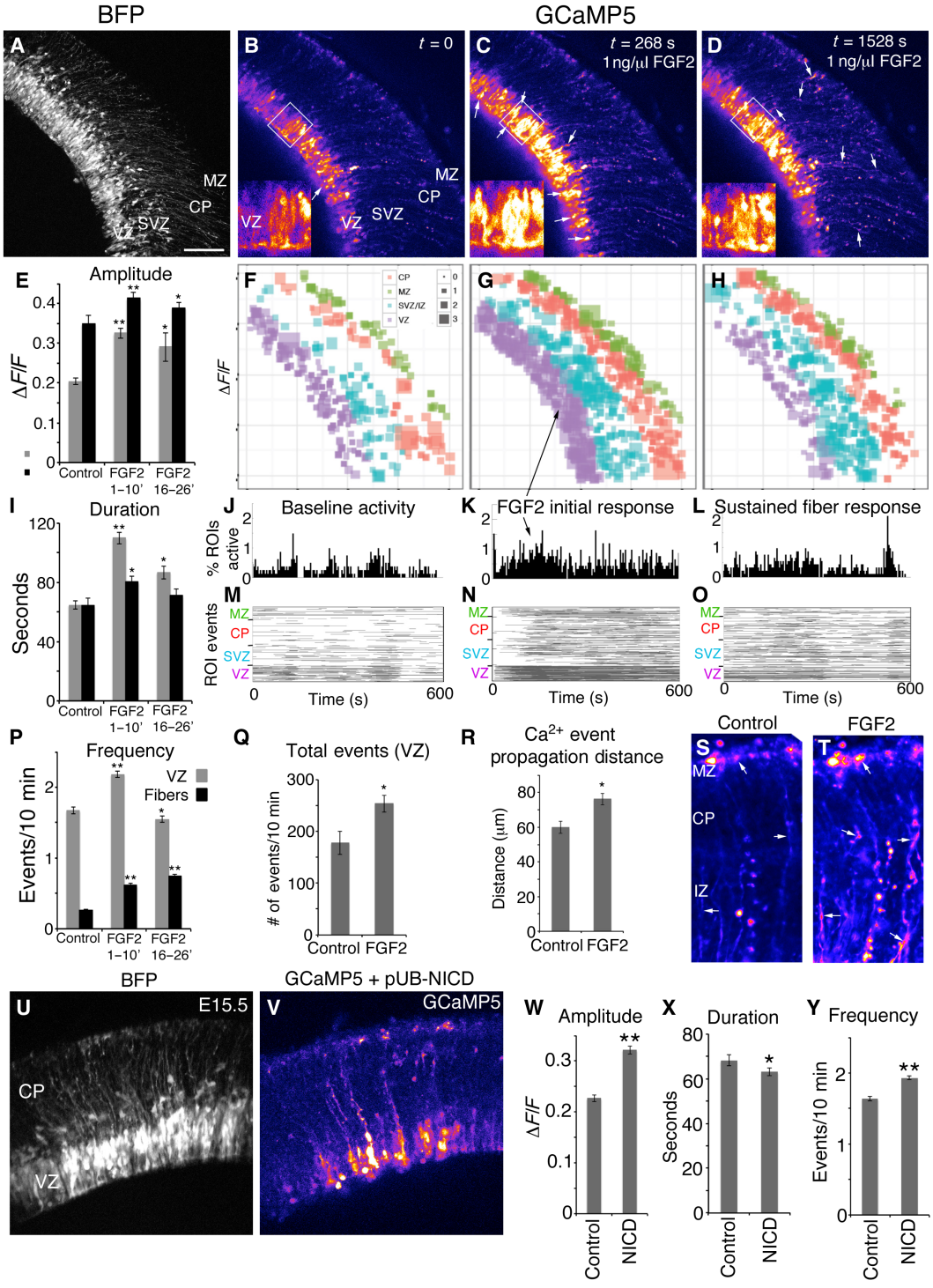

Fig. 5. Calcium activity induced by FGF2 and Notch. (**A**) BFP Z-stack of an E15.5 cortical slice. (**B**) Baseline calcium activity. (**C** and **D**) Calcium activity after FGF2 exposure; inset panels are high-magnification images of boxed region. (**E**, **I**, and **P**) Δ*F/F* amplitude, duration, and frequency of Ca^{2+} events in RGC cell bodies and fibers under control conditions, after initial FGF2 exposure, and sustained FGF2 exposure. (**F** to **H**) Δ*F/F* amplitude of active ROIs plotted spatially; square size represents relative amplitude. (**J** to **L**) Percentages of ROIs active. (**M** to **O**) Rasterplots of all detected Ca^{2+} events binned according to embryonic zone (VZ, SVZ, CP, and MZ). (**Q**) Total number of events in the VZ. (**R**) Ca^{2+} event propagation distance within RGC fibers. (**S** and **T**) Averaged movies show accumulated Ca^{2+} activity within RGC fibers and end feet in 400-s epochs. (**U**) BFP Z-stack of an E15.5 slice coexpressing GCaMP5G and Notch intracellular domain (NICD). (**V**) GCaMP5 Ca^{2+} signal. (**W** to **Y**) Effects of NICD overexpression on Ca2+ event properties of RGC cell bodies. *$P < 0.05$; **$P < 0.001$, *t* test. Error bars, mean ± SEM. Scale bar, 100 μm (A to D, U, and V) and 50 μm in insets of (B) to (D), (S), and (T).

DISCUSSION

Radial communication of an unknown kind has been hypothesized for decades to influence the development of cortical columns (*4*, *6*). Indeed, the eventual deposition of excitatory cortical neurons into the correct layers requires instructive cues and positional information in the radial dimension. Here, we found a novel mode of intercellular, propagative Ca^{2+} activity that allows an exchange of information along the migratory pathway of developing neurons and appears to play a role in regulating cortical column development.

The core of this mechanism is long-range, bidirectional radial Ca^{2+} activity propagation via the RGC fiber. We found that Ca^{2+} transient events were initiated in RGC fibers and represent an independent source of calcium activity that propagates to and activates RGC cell bodies. Thus, RGC fibers initiate and partly regulate the level of Ca^{2+} activity in cortical progenitor somata. We further found that migrating neurons maintain direct communication with RGC progenitors during the early stages of their radial migration along RGC fibers. Bursts of Ca^{2+} activity in migrating neurons, some of which is imparted by RGC fiber Ca^{2+} activity, appeared to induce saltatory migratory movements, in essence providing a motivational force to exit the proliferative zones and, in principle, reach appropriate cortical layers on schedule. Our data are consistent with the hypothesis that Ca^{2+} bursting in differentiating RGCs is necessary for neurogenesis and/or neuronal VZ exit because Notch hyperactivation suppressed both Ca^{2+} bursting and neurogenesis, whereas inhibition of IP_3R-mediated Ca^{2+} release via 2-APB exposure produced an apparent phenocopy. Thus, Notch-dependent regulation of cortical cell fate likely involves a downstream Ca^{2+} modulatory mechanism.

Therefore, we suggest that radially propagative activity in RGC fibers allows progenitors in the VZ, SVZ, and oSVZ (outer SVZ) to communicate and coordinate proliferation and neurogenesis, whereas the independent Ca^{2+} activity generated in RGC fibers within the CP amounts to a feedback mechanism, permitting the developing CP to influence progenitor activities. Such feedback increases the baseline Ca^{2+} "tone" of progenitor cells.

Our data indicate that elevated Ca^{2+} activity may be important for progenitor proliferation, neurogenesis, and neuronal exit from the VZ and illustrate how a single type of cellular dynamic process can be needed at specific stages for the proper regulation of multiple developmental mechanisms. The frequency/amplitude gradient of Ca^{2+} activity within RGC fibers indicates that migrating cortical neurons are provided with positional information on their radial location within cortical columns, which we suggest may help neurons settle in the correct layer. Our observation of clusters of RGC fibers with synchronous activity strongly indicates that cortical columns do not necessarily arise through the influence of individual RGC fibers but can also involve small groups acting together. In this "honeycomb" model of column development, RGCs cooperate in column development as members of a local group defined by a shared activation mechanism. We speculate that coherent activity in clusters of RGCs may locally synchronize the neurogenesis and exit of newborn cortical neurons from the VZ. In principle, synchronized Ca^{2+} activity during neurogenesis could provide a basis for regulating the cytoarchitecture of individual columns.

The tight correlation of neurogenesis with Ca^{2+} bursting shows that high-frequency Ca^{2+} activity is an integral component of apical end-foot retraction and initial neuronal differentiation during protocolumn formation. In the VZ, excess Notch signaling—well known to prevent neuronal differentiation (*43*)—increased general Ca^{2+} activity in the RGC pool but effectively abolished the Ca^{2+} bursting associated with newborn neurons, suggesting that a frequency threshold must be reached to induce neuronal exit of the stem cell niche. Inhibition of IP_3R-mediated release by 2-APB also abolished calcium bursting and associated VZ exit. Thus, we demonstrate Ca^{2+} dependence of a key neuronal commitment stage—the physical exit from the stem cell niche—which isolates the neuroblast from stem cell factors in the VZ and embryonic cerebrospinal fluid that are important for cortical stem cell activities (*44*).

Classic morphogens such as FGF8 regulate the tangential patterning of the protomap and hence the size and distribution of cortical areas (*9*, *10*). However, our results add a new dimension to their function in that FGF and Notch activities appear to have roles in cortical column development through their regulation of RGC Ca^{2+} signaling and downstream Ca^{2+}-dependent processes within the radial scaffold. Conceptually, the areal patterning mechanisms via FGF activity are therefore coupled to cortical column development through radial Ca^{2+} signaling, providing insight into how the cytoarchitecture of different functional areas can be achieved.

Thicker cortices (for example, primate) would be expected to be more dependent on such radial communication mechanisms because the distances neurons must migrate are substantially longer. In this respect, genetic or environmental disruptions in the interaction of morphogenetic factors and Ca^{2+} activity and consequent effects on RGCs and newborn neurons could create additional opportunities for malformations in primate cortical columns. It may be difficult to predict which environmental factors or maternal medications could alter these Ca^{2+} signals because factors that modulate FGF or Notch activity, for example, and not just agents that interfere with Ca^{2+} channels, can change Ca^{2+} activity patterns. In conclusion, our study indicates that the establishment of the complex columnar and laminar organization of the cerebral cortex involves radial, Ca^{2+}-dependent communication that is regulated by morphogenetic signaling systems, including FGF and Notch, well before the onset of synaptogenesis.

MATERIALS AND METHODS

Animals and IUE

Animal procedures were performed in accordance with the policies of the Yale Institutional Care and Use Committee. A total of 86 timed-pregnant CD-1 mice were purchased from Charles River Laboratories and housed at the Yale Sterling Hall of Medicine animal facility. Pregnant dams were anesthetized by ketamine/xylazine intraperitoneal injection, and IUE was performed as described previously (*37*). A total of 267 embryos were coelectroporated with pCAG-GCaMP5 (Addgene) and pCAG-BFP together, or in combination of pUb-NICD (J. J. Breunig), at embryonic stages ranging from E10.5 to E16.5 and allowed to develop in utero for varying lengths of time until calcium imaging of embryos extracted from the mother in ice-cold, oxygenated ACSF (125 mM NaCl, 5 mM KCl, 1.25 mM NaH_2PO_4, 1.25 mM $MgCl_2$, 2 mM $CaCl_2$, 25 mM $NaHCO_3$, and 10 mM dextrose) bubbled with 95% O_2 and 5% CO_2.

Immunohistochemistry and tissue processing

Embryonic brains were immersion-fixed in 4% paraformaldehyde overnight. Thin (25-μm) sections were prepared using a cryostat (Leica

Microsystems). Immunohistochemistry was performed as described previously (*37*); antibody species and concentrations were Pax6 (Abcam, rabbit, 1:1000) and Tbr2 (Abcam, chicken, 1:500).

Ex vivo imaging

The cortical wall was electroporated at E10.5, and embryos were allowed to survive in utero for 12 hours. The embryos were removed from the mother and immediately dissected in ice-cold, oxygenated ACSF. Intact, living embryos (identified by the presence of a heartbeat) were then submerged in a glass-bottom petri dish (MatTek) mounted on a heated stage with a heated ACSF delivery and aspiration system (Warner Instruments) mounted on an inverted Zeiss 510 Meta confocal microscope with a titanium-sapphire two-photon laser (Coherent). The embryos were kept at 37°C during the imaging session. BFP *Z*-stacks were acquired at 780-nm excitation using the two-photon laser, whereas GCaMP5 movies were acquired under 488-nm argon laser excitation at 1024 × 1024 resolution. An LP505 emission filter was used to collect the maximum emitted light. At E11.0, the cortical wall and overlying ectoderm and mesenchyme are thin enough (about 200 μm) to allow single-cell resolution in calcium movies. Two-photon *Z*-stacks of BFP-labeled neuroepithelial cells showed the detailed cellular morphology of analyzed cells.

Live slice imaging

Electroporated embryos were harvested and euthanized by decapitation, and the brains were quickly dissected and placed into ice-cold, oxygenated ACSF. The brains were embedded in 3.2% select agar (Sigma) in phosphate-buffered saline, and 250-μm slices were quickly made on a Leica VT1000S vibrating microtome and then placed in oxygenated ACSF to recover at room temperature for 20 min. The slices were then kept up to 24 hours in ice-cold, oxygenated ACSF until imaging. The imaging depth was a minimum of 20 μm to avoid damaged cells near the slice surface. FGF2 protein (Invitrogen), 2-APB (Sigma), and PD173074 (Abcam) were dissolved in oxygenated ACSF immediately before bath application and imaging. Movies were acquired at scan rates ranging from 1 to 0.25 Hz with 1024 × 1024 or 2048 × 2048 resolution, and the slices were imaged for up to 4 hours, after which they began to degrade.

Calcium signal detection

Image processing and calcium signal detection were performed using ImageJ [National Institutes of Health (NIH)], and custom software routines were written in MATLAB (MathWorks) (*11*). A motion correction algorithm implemented with the StackReg plugin was first applied to the movie to correct for small *X*-*Y* displacements within the focal plane. The cell contours corresponding to cell bodies, fibers, end feet, or other cellular regions were semiautomatically identified in the average image, F_0, and an ROI mask created around each cellular element. ROIs were binned by user-defined anatomical regions corresponding to the VZ, SVZ/IZ, CP, and MZ. Calcium signals for each ROI were defined as deviations from the average fluorescence intensity inside each ROI in each frame, *Ft*, measured as a function of time ($\Delta F/F = (Ft - F_0)/F_0$). Calcium events were extracted using automatic detection routines confirming events as local maxima (>2 SDs of the derivative of the signal). The movie segments containing drift out of the field of focus were excluded from calcium event detection. Calcium event onsets were set as the first frame in the rising phase of the signal. Event offsets were set as the half-amplitude decay time for each calcium transient. Calcium bursting was defined by either a continuous or discontinuous calcium transient frequency of ≥5 calcium events with greater than 20% $\Delta F/F$ in a 4-min epoch. In a slice subset analysis ($N = 8$ slices), a total of 3528 VZ events from 1609 ROIs and a total of 2489 events from 4868 fiber ROIs were analyzed. On a per-slice basis, an average of 201.1 ± 14.3 ROIs exhibiting 441.0 ± 61.8 calcium events in the VZ (RGC cell bodies) and 608.5 ± 44.3 ROIs exhibiting 311.1 ± 47.6 calcium events collectively in the SVZ/IZ, CP, and MZ (RGC fiber events) were analyzed in each 26-min movie using custom scripts in MATLAB. Event/ROI ratios were 2.19 ± 0.274 for VZ ROIs and 0.526 ± 0.08 for fiber ROIs. Assuming a 1:1 ratio for RGC fibers and cell bodies, the normalized ratio of events per fiber was approximately 1.59 ± 0.242 events per RGC fiber per 26-min movie. Because MATLAB relies on static ROIs for its analysis, the $\Delta F/F$ traces of migrating neurons were constructed by manually shifting the position of an ROI over a neuron as it migrates.

Data analysis

Data sets were analyzed using custom routines written in MATLAB (MathWorks) and in R (The R Project for Statistical Computing, www.r-project.org). Calcium event properties (amplitude, duration, and frequency) were extracted using the event onset and offset times in the data time series for each ROI of each recording and used for population-level analysis. Active ROIs were ROIs exhibiting at least one calcium event during a recording period. Peak coactive network activity was quantified as the maximum percentage of cells exhibiting a calcium event at one time during a recording period. Brightness plots were constructed using ImageJ to extract average brightness intensities of user-defined ovoid ROIs. To quantify temporal correlations between pairs of ROIs within a recording, a correlation measure was computed from the inner product of the event onset vectors (with each calcium event having a window of ±1 frame of the detected event onset) for each pair of ROIs in a recording. Monte Carlo simulations of the event onset vectors were then performed, where the significance of the observed correlation measure was determined through comparison with distributions calculated from 1000 randomized data sets using a threshold significance level of $P < 0.01$. Distribution means were compared using two-sample Student's *t* tests or using analysis of variance (ANOVA) followed by pairwise *t* tests with Holm correction when analyzing the effects of multiple grouping factors ($P < 0.05$ set as significance). Values are reported as means with the SEM or medians with the median absolute deviation.

SUPPLEMENTARY MATERIALS

Supplementary material for this article is available at http://advances.sciencemag.org/cgi/content/full/2/2/e1501733/DC1

Fig. S1. Conduction of an RGC cell body–initiated calcium transient to apical and pial end feet.
Fig. S2. An inverse amplitude/frequency relationship in RGC fibers.
Fig. S3. Neurons exhibit decreased calcium transient activity at later stages of migration.
Fig. S4. Calcium transients in cortical progenitors at E11.0 ex vivo.
Fig. S5. Calcium activity reduced by the FGFR antagonist PD173074.
Video S1. Calcium transients are initiated within RGC fibers and propagate bidirectionally.
Video S2. Burst Ca^{2+} transients in RGC fibers reveal frequency modulation.
Video S3. RGC somata initiate anterograde and receive retrograde PCTs.
Video S4. An RGC somal Ca^{2+} transient reaches the pial surface.
Video S5. A retrograde Ca^{2+} transient activates an RGC soma.
Video S6. Retrograde propagation of Ca^{2+} activity initiated at a pial end foot.
Video S7. Coherent activity in RGC fiber clusters.
Video S8. Simultaneous activation of RGC pial end feet.

Video S9. Apparent RGC fiber-fiber transmission in the IZ/CP.
Video S10. Calcium burst activity during apical end-foot retraction.
Video S11. Impairment of Ca^{2+} activity by 2-APB reduces RGC motility.
Video S12. Calcium burst activity during initial neuronal migration.
Video S13. En passant Ca^{2+} activity in an RGC fiber repeatedly induces a neuronal Ca^{2+} response.
Video S14. En passant Ca^{2+} activity in an RGC fiber induces a neuronal Ca^{2+} response.
Video S15. Ex vivo Ca^{2+} transient activity at E11.0.
Video S16. Baseline Ca^{2+} activity before FGF2 application.
Video S17. FGF2 induces Ca^{2+} activity in RGCs.
Video S18. Baseline Ca^{2+} activity before FGF2 application.
Video S19. Increased PCTs in RGC fibers after FGF2 exposure.
Video S20. Notch activation increases Ca^{2+} activity in RGCs but reduces bursting associated with neurogenesis.

REFERENCES AND NOTES

1. V. B. Mountcastle, The columnar organization of the neocortex. *Brain* **120**, 701–722 (1997).
2. P. Rakic, Specification of cerebral cortical areas. *Science* **241**, 170–176 (1988).
3. S. C. Noctor, A. C. Flint, T. A. Weissman, R. S. Dammerman, A. R. Kriegstein, Neurons derived from radial glial cells establish radial units in neocortex. *Nature* **409**, 714–720 (2001).
4. P. Rakic, Evolution of the neocortex: A perspective from developmental biology. *Nat. Rev. Neurosci.* **10**, 724–735 (2009).
5. M. Torii, K. Hashimoto-Torii, P. Levitt, P. Rakic, Integration of neuronal clones in the radial cortical columns by EphA and ephrin-A signalling. *Nature* **461**, 524–528 (2009).
6. C. Dehay, H. Kennedy, Cell-cycle control and cortical development. *Nat. Rev. Neurosci.* **8**, 438–450 (2007).
7. J. H. Lui, D. V. Hansen, A. R. Kriegstein, Development and evolution of the human neocortex. *Cell* **146**, 18–36 (2011).
8. P. Rakic, Neurons in rhesus monkey visual cortex: Systematic relation between time of origin and eventual disposition. *Science* **183**, 425–427 (1974).
9. T. Fukuchi-Shimogori, E. A. Grove, Neocortex patterning by the secreted signaling molecule FGF8. *Science* **294**, 1071–1074 (2001).
10. S. Garel, K. J. Huffman, J. L. R. Rubenstein, Molecular regionalization of the neocortex is disrupted in *Fgf8* hypomorphic mutants. *Development* **130**, 1903–1914 (2003).
11. J. B. Ackman, T. J. Burbridge, M. C. Crair, Retinal waves coordinate patterned activity throughout the developing visual system. *Nature* **490**, 219–225 (2012).
12. J. B. Ackman, M. C. Crair, Role of emergent neural activity in visual map development. *Curr. Opin. Neurobiol.* **24**, 166–175 (2014).
13. A. Shitamukai, D. Konno, F. Matsuzaki, Oblique radial glial divisions in the developing mouse neocortex induce self-renewing progenitors outside the germinal zone that resemble primate outer subventricular zone progenitors. *J. Neurosci.* **31**, 3683–3695 (2011).
14. M.-R. Rašin, V.-R. Gazula, J. J. Breunig, K. Y. Kwan, M. B. Johnson, S. Liu-Chen, H.-S. Li, L. Y. Jan, Y.-N. Jan, P. Rakic, N. Šestan, Numb and Numbl are required for maintenance of cadherin-based adhesion and polarity of neural progenitors. *Nat. Neurosci.* **10**, 819–827 (2007).
15. K. Bittman, D. F. Owens, A. R. Kriegstein, J. J. LoTurco, Cell coupling and uncoupling in the ventricular zone of developing neocortex. *J. Neurosci.* **17**, 7037–7044 (1997)
16. T. F. Haydar, F. Wang, M. L. Schwartz, P. Rakic, Differential modulation of proliferation in the neocortical ventricular and subventricular zones. *J. Neurosci.* **20**, 5764–5774 (2000)
17. T. A. Weissman, P. A. Riquelme, L. Ivic, A. C. Flint, A. R. Kriegstein, Calcium waves propagate through radial glial cells and modulate proliferation in the developing neocortex. *Neuron* **43**, 647–661 (2004).
18. X. Liu, K. Hashimoto-Torii, M. Torii, C. Ding, P. Rakic, Gap junctions/hemichannels modulate interkinetic nuclear migration in the forebrain precursors. *J. Neuroci.* **30**, 4197–4209 (2010).
19. S. Malmersjö, P. Rebellato, E. Smedler, P. Uhlén, Small-world networks of spontaneous Ca^{2+} activity. *Commun. Integr. Biol.* **6**, e24788 (2013).
20. S. E. Webb, A. L. Miller, Calcium signalling during embryonic development. *Nat. Rev. Mol. Cell Biol.* **4**, 539–551 (2003).
21. M. J. Berridge, The versatility and complexity of calcium signalling. *Novartis Found. Symp.* **239**, 52–64 (2001).
22. N. C. Spitzer, Electrical activity in early neuronal development. *Nature* **444**, 707–712 (2006).
23. T. M. Gomez, N. C. Spitzer, In vivo regulation of axon extension and pathfinding by growth-cone calcium transients. *Nature* **397**, 350–355 (1999).
24. R. O. L. Wong, A. Ghosh, Activity-dependent regulation of dendritic growth and patterning. *Nat. Rev. Neurosci.* **3**, 803–812 (2002).
25. L. Cancedda, H. Fiumelli, K. Chen, M.-m. Poo, Excitatory GABA action is essential for morphological maturation of cortical neurons in vivo. *J. Neurosci.* **27**, 5224–5235 (2007).
26. A. K. McAllister, Cellular and molecular mechanisms of dendrite growth. *Cereb. Cortex* **10**, 963–973 (2000).
27. H. T. Cline, Dendritic arbor development and synaptogenesis. *Curr. Opin. Neurobiol.* **11**, 118–126 (2001)
28. J. Akerboom, T.-W. Chen, T. J. Wardill, L. Tian, J. S. Marvin, S. Mutlu, N. C. Calderón, F. Esposti, B. G. Borghuis, X. R. Sun, A. Gordus, M. B. Orger, R. Portugues, F. Engert, J. J. Macklin, A. Filosa, A. Aggarwal, R. A. Kerr, R. Takagi, S. Kracun, E. Shigetomi, B. S. Khakh, H. Baier, L. Lagnado, S. S.-H. Wang, C. I. Bargmann, B. E. Kimmel, V. Jayaraman, K. Svoboda, D. S. Kim, E. R. Schreiter, L. L. Looger, Optimization of a GCaMP calcium indicator for neural activity imaging. *J. Neurosci.* **32**, 13819–13840 (2012).
29. E. K. Stancik, I. Navarro-Quiroga, R. Sellke, T. F. Haydar, Heterogeneity in ventricular zone neural precursors contributes to neuronal fate diversity in the postnatal neocortex. *J. Neurosci.* **30**, 7028–7036 (2010).
30. N. C. Spitzer, Neuroscience: A bar code for differentiation. *Nature* **458**, 843–844 (2009).
31. A. S. Freitas, A. L. R. Xavier, C. M. Furtado, C. Hedin-Pereira, M. M. Fróes, J. R. L. Menezes, Dye coupling and connexin expression by cortical radial glia in the early postnatal subventricular zone. *Dev. Neurobiol.* **72**, 1482–1497 (2012).
32. K. S. Bittman, J. J. LoTurco, Differential regulation of connexin 26 and 43 in murine neocortical precursors. *Cereb. Cortex* **9**, 188–195 (1999).
33. P. Rakic, Mode of cell migration to the superficial layers of fetal monkey neocortex. *J. Comp. Neurol.* **145**, 61–83 (1972).
34. S. C. Noctor, V. Martínez-Cerdeño, L. Ivic, A. R. Kriegstein, Cortical neurons arise in symmetric and asymmetric division zones and migrate through specific phases. *Nat. Neurosci.* **7**, 136–144 (2004).
35. H. Komuro, P. Rakic, Intracellular Ca^{2+} fluctuations modulate the rate of neuronal migration. *Neuron* **17**, 275–285 (1996)
36. H. Shimojo, T. Ohtsuka, R. Kageyama, Oscillations in notch signaling regulate maintenance of neural progenitors. *Neuron* **58**, 52–64 (2008).
37. B. G. Rash, H. D. Lim, J. J. Breunig, F. M. Vaccarino, FGF signaling expands embryonic cortical surface area by regulating Notch-dependent neurogenesis. *J. Neurosci.* **31**, 15604–15617 (2011).
38. B. G. Rash, S. Tomasi, H. D. Lim, C. Y. Suh, F. M. Vaccarino, Cortical gyrification induced by fibroblast growth factor 2 in the mouse brain. *J. Neurosci.* **33**, 10802–10814 (2013).
39. S. D. Skaper, W. J. Kee, L. Facci, G. Macdonald, P. Doherty, F. S. Walsh, The FGFR1 inhibitor PD 173074 selectively and potently antagonizes FGF-2 neurotrophic and neurotropic effects. *J. Neurochem.* **75**, 1520–1527 (2000).
40. B. G. Rash, E. A. Grove, Area and layer patterning in the developing cerebral cortex. *Curr. Opin. Neurobiol.* **16**, 25–34 (2006).
41. F. M. Vaccarino, M. L. Schwartz, R. Raballo, J. Nilsen, J. Rhee, M. Zhou, T. Doetschman, J. D. Coffin, J. J. Wyland, Y.-T. E. Hung, Changes in cerebral cortex size are governed by fibroblast growth factor during embryogenesis. *Nat. Neurosci.* **2**, 848 (1999).
42. C. Blanpain, W. E. Lowry, H. A. Pasolli, E. Fuchs, Canonical notch signaling functions as a commitment switch in the epidermal lineage. *Genes Dev.* **20**, 3022–3035 (2006).
43. R. Kageyama, T. Ohtsuka, H. Shimojo, I. Imayoshi, Dynamic Notch signaling in neural progenitor cells and a revised view of lateral inhibition. *Nat. Neurosci.* **11**, 1247–1251 (2008).
44. M. K. Lehtinen, M. W. Zappaterra, X. Chen, Y. J. Yang, A. D. Hill, M. Lun, T. Maynard, D. Gonzalez, S. Kim, P. Ye, A. J. D'Ercole, E. T. Wong, A. S. LaMantia, C. A. Walsh, The cerebrospinal fluid provides a proliferative niche for neural progenitor cells. *Neuron* **69**, 893–905 (2011).

Acknowledgments: We dedicate this paper to the memory of Vernon Mountcastle (1918–2015) who discovered the existence of cortical columns and recognized their significance as the working units of the mind. We are grateful to A. Ayoub for help with the confocal slice culture setup and two-photon imaging, as well as helpful discussions. We thank H. Komuro, J. Arellano, and A. Duque for helpful discussions and critical reading of the manuscript. **Funding:** We are grateful for funding by the Kavli Institute for Neuroscience at Yale University and NIH grants DA023999, NS014841, and R01EY002593 (to P.R.). **Author contributions:** B.G.R. designed and conducted research and analyzed data. J.B.A. and B.G.R. designed and wrote custom scripts in MATLAB and R to extract and process data from calcium movies. J.B.A. edited the manuscript. P.R. designed research and supervised the project. B.G.R. and P.R. wrote the paper. **Competing interests:** The authors declare that they have no competing interests. **Data and materials availability:** All data needed to evaluate the conclusions in the paper are present in the paper and/or the Supplementary Materials. Additional data related to this paper may be requested from the authors.

Submitted 30 November 2015
Accepted 17 December 2015
Published 26 February 2016
10.1126/sciadv.1501733

Citation: B. G. Rash, J. B. Ackman, P. Rakic, Bidirectional radial Ca^{2+} activity regulates neurogenesis and migration during early cortical column formation. *Sci. Adv.* **2**, e1501733 (2016).